Pharm Res (2011) 28:788–796
DOI 10.1007/s11095-010-0332-2

RESEARCH PAPER

Formation of Protein Nano-Matrix Particles with Controlled Surface Architecture for Respiratory Drug Delivery

Philip Chi Lip Kwok • Amolnat Tunsirikongkon • William Glover • Hak-Kim Chan

Received: 10 August 2010 / Accepted: 17 November 2010 / Published online: 7 December 2010

ABSTRACT

Purpose To produce and examine the aerosol performance of protein nano-matrix particles with different surface roughness.

Methods Aqueous lysozyme solutions were poured into isopropanol during high-shear mixing to produce nanoparticles by precipitation. The size of the nanoparticles was varied by adjusting the precipitation conditions. The resultant suspensions were spray-dried to obtain micron-sized aggregates (nano-matrices). Smooth particles were made by spray-drying a lysozyme solution. The aggregate size distribution, surface roughness, and cohesion were evaluated. The aerosol performance was assessed by dispersing 10 mg of powder from a Rotahaler® at 60 L/min or an Aerolizer® at 100 L/min into a Next Generation Impactor, followed by chemical assay ($n = 3$).

Results The median volume diameter and span of the nano-matrix particles were 1.0–1.2 μm and 1.5–1.6, respectively, which were comparable to those of the smooth particles. Surface roughness increased with the size of the primary nanoparticles. The nano-matrix particles were significantly less cohesive than the smooth particles. The fine particle fraction increased linearly with increasing surface roughness and decreasing cohesion.

Conclusions Nano-matrix particles with controlled surface architecture were successfully produced by spray-drying nanosuspensions. Aerosol performance was enhanced with increasing surface roughness due to the reduction in cohesion forces.

KEY WORDS aggregates · dispersion · lysozyme
nano-matrix · roughness

INTRODUCTION

Pharmaceutical inhalation aerosols offer the distinct advantage of rapid and convenient delivery of drugs to the site of action, as exemplified by the traditional administration of bronchodilators for asthma treatment. More recently, driven by the pharmaceutical industry to explore the potential of the lungs for systemic treatment of diseases, pulmonary drug delivery by inhalation aerosols has been undergoing rapid and intense development (1). Biotechnology-derived potent drugs have been successfully delivered to the lungs, for instance, rhDNase for the treatment of cystic fibrosis and, most recently, insulin for diabetes (2,3). In response to the increased level of interest in the delivery of biologically active materials via the pulmonary route, significant research effort has been directed towards the development of innovative technologies for the generation of dry powder aerosols for inhalation.

A dry powder inhaler (DPI) product comprises a powder formulation loaded to an inhaler device. Drugs marketed for DPI are usually prepared as micron-sized particles (< 5 μm) (4). These particles are conventionally produced by crystal-

P. C. L. Kwok • H.-K. Chan (✉)
Advanced Drug Delivery Group, Faculty of Pharmacy
The University of Sydney
Building A15
Camperdown, NSW 2006, Australia
e-mail: kim.chan@sydney.edu.au

A. Tunsirikongkon
Department of Pharmaceutics and Industrial Pharmacy
Faculty of Pharmaceutical Sciences
Chulalongkorn University
Phyathai Road, Patumwan
Bangkok 10330, Thailand

W. Glover
GSK Consumer Health
82 Hughes Avenue
Ermington, NSW 2115, Australia

lisation followed by milling in the pharmaceutical industry. However, milling produces particles that are usually cohesive, partially amorphous and physically unstable (5), making powder deagglomeration and precise delivery to the lungs difficult.

The traditional formulation approach for DPIs is to blend the drug particles with a large quantity (>95%) of coarse (e.g. 90–120 μm) carrier particles of lactose, to improve the powder handling properties (e.g. flowability) and aerosol performance of cohesive drugs (6). For high-dose drugs, blends become impractical, as the amount will be too large to inhale, leading to airway irritation or coughing. A more recent formulation approach is to reduce the inter-particulate forces through the use of corrugated drug particles (7). Small variations in the surface roughness were shown to produce significant performance variations in the powders of bovine serum albumin (BSA) (8–11). These corrugated particles were produced by spray-drying the drug solutions. However, the use of solutions is limited, as it depends on the solubility of the drugs. Furthermore, since the drying is fast (in the order of seconds), particle formation in the droplets and the resulting surface roughness of the particles is not easy to predict. So far, corrugated particles of mainly amorphous materials such as BSA have been attained. For crystalline materials, the surface roughness of the particles is even less controllable, as it will be predominated by the crystal structure.

We propose to control the particle surface roughness using nanosuspensions for the spray-drying process. Nanomedicine is a rapidly expanding research area but has been largely unexplored for pharmaceutical aerosols (12). Nanoparticles have high specific surface area; thus, they may enhance the dissolution and, consequently, the bioavailability of sparingly soluble drugs. Since the optimal aerodynamic diameter for pulmonary peripheral deposition is 1–3 μm (13), the nanoparticles are usually formulated as micron-sized aggregates instead of loose primary particles. Large hollow aggregates with geometric diameters >5 μm have been produced by spray-drying nanosuspensions (14–16). The nanoparticles may be loaded with drugs and other excipients during preparation. Tsapis *et al.* (14) employed non-biocompatible nanoparticles (silica and polystyrene), which have limited clinical applications. On the other hand, Gómez-Gaete *et al.* (16) and Hadinoto *et al.* (15) used biodegradable poly (D,L-lactide-co-glycolide) (PLGA) and polyacrylate loaded with drugs. The aerodynamic diameter of the hollow aggregates is within inhalable range due to their low density. These aggregates are designed to be drug carriers that disintegrate into the primary nanoparticles after deposition upon the lung fluid lining (14). The drug release rate is related to the aggregate porosity (15). Disintegration of the nanoparticle aggregates can be actively promoted by formulating with effervescence agents such as sodium carbonate and citric acid (17–19). The effervescent reaction occurs when the aggregates are exposed to high humidity in the airways and produces carbon dioxide, which actively disintegrates the aggregates and releases the primary particles (17–19). Since nanoparticles can diffuse into tumours, spray-freeze-dried aggregates loaded with anticancer agents have been formulated. Thus, drug targeting is more precise, and toxic effects are reduced (20,21). Improvement in drug delivery is also due to the fact that nanoparticles are not susceptible to mucociliary clearance; thus, their presence at the site of deposition is lengthened (22).

The applications discussed above focused on the redispersion of the nanoparticles and the enhancement or control of drug release. The formulations require a range of excipients to form the nanoparticles and aggregate matrix. The base material of the primary particles is usually polymeric. A simpler approach is to produce nano-sized drug particles and then transform them into aggregates. Loose agglomerates have been formed with single drugs (23–25) or combination actives (26,27) by anti-solvent precipitation followed by freeze-drying. Surfactants and polymers were included as nanoparticle stabilisers. The resultant agglomerates were within the inhalable size range and produced respiratory fractions >75% of the total dose at an air-flow rate of 30 L/min (23–27). The aerosol performance was exceptionally good, given that the air-flow rate is relatively low and no inhalers were used in the impaction with the Tisch Ambient Cascade Impactor. These agglomerates were loose and irregular in shape (24–27). The surface morphology between agglomerates also differed quite markedly (25), probably because aggregate shape is difficult to control in freeze-drying. On the other hand, the drying of nanosuspension droplets yielded spheroidal aggregates. For example, silica colloidal suspensions sprayed from an ultrasonic nebuliser produced regular, ball-like clusters after drying (28). The surface roughness of these aggregates increased with the size of the nanoparticles (28). However, aerosol performance was not assessed in this study, as silica is not intended to be inhaled. Spray-drying is a simple one-step process for the production of pharmaceutical powders. Micron-sized spheroidal clusters (median volume diameter of 1–3 μm) have been produced from drug nanosuspensions using this technique (29–32). Thus, it is well suited for controlling the size and surface architecture of nano-matrix particles in the present study.

Recently, it has become feasible to produce nanoparticles of pure drugs in large-scale quantities by precipitation (30,33). These nanoparticles have a potential to provide the ideal

building blocks for fabrication of particles with preferred architectures. The micron-sized aggregates (termed 'nano-matrix particles' in this paper) obtained from spray-drying the nano-precipitates were shown to have high aerosol performance (29,30,34). However, much remains to be done to develop this novel particle engineering process for controlling particle surface architecture at the nano-scale. In the present study, by changing the primary size of the nanoparticles, we produced nano-matrix particles with controlled surface roughness and investigated their interparticulate force and aerosol performance.

MATERIALS AND METHODS

Preparation of Nano-Matrix and Smooth Particles

The nano-matrix particles of lysozyme (L6876 lysozyme from chicken egg white; Sigma-Aldrich, Castle Hill, Australia) as a model protein drug were produced by spray-drying of suspensions containing the primary nanoparticles of the protein. Primary nanoparticles were produced by anti-solvent precipitation as follows. An aqueous solution of lysozyme was quickly poured into a known volume of isopropanol (Lomb Scientific, Taren Point, Australia) in a 600 mL beaker being stirred at 6000 rpm using a Silverson Model L4RT high-shear mixer with a 0.75 inch tubular mixing assembly and general purpose disintegrating head (Silverson Machines, Chesham, UK), resulting in immediate precipitation. Depending on the formulation, the resulting suspension was spray-dried with or without further dilution with isopropanol, to produce the nano-matrix particles. Three formulations were used, and the details are given in Table I. Smooth lysozyme particles were obtained by spray-drying an aqueous solution of 4 mg/mL lysozyme.

All samples were spray-dried with a Büchi Mini Spray Dryer B-290 (Büchi Labortechnik, Flawil, Switzerland) under the same operating conditions. The spray-dryer was connected to a Büchi Dehumidifier B-296 and Büchi Inert Loop B-295 (in closed loop, blowing mode for organic solvent spray-drying). The operation conditions were as follows: liquid feed rate at 5.4 mL/min, inlet and outlet temperatures at 80°C and 64°C, respectively, aspirator at 100% (i.e. 38 m^3/h), and atomising air flow at 819 NL/h.

Scanning Electron Microscopy

Particle surface morphology was imaged by field emission scanning electron microscopy (SEM) at 5 kV (Zeiss Ultra Plus; Carl Zeiss, Oberkochen, Germany). The resolution at this acceleration voltage is 1.5 nm (35). The samples were dispersed onto carbon sticky tabs and sputter-coated with approximately 15 nm gold before imaging.

Dynamic Light Scattering

The nanoparticles were sized by dynamic light scattering before spray-drying (Malvern Zetasizer Nano ZS; Malvern, Worcestershire, UK). The measurement parameters were as follows: the refractive indices for lysozyme and isopropanol were 1.445 and 1.390, respectively, the absorption value of lysozyme was 0.1, and the viscosity of isopropanol was 2.32 mPa·s. The samples were measured in a quartz cuvette at 25°C. Particle size distributions were measured in triplicates ($n=3$).

Laser Diffraction

Size distribution of the nano-matrix and smooth particles was determined by laser diffraction (Malvern Mastersizer 2000 with Hydro SM small volume sample dispersion unit; Malvern, Worcestershire, UK). Approximately 5 mg of sample was sonicated in 2 mL isopropanol for 1 min in an ultrasonic water bath (Model FXT8; Unisonics Australia, Brookvale, NSW, Australia). Particle size distributions were measured between an obscuration of 4–6% in triplicates ($n=3$). The measurement parameters were as follows: the refractive indices for lysozyme and isopropanol were 1.445 and 1.390, respectively, and the absorption value of lysozyme was 0.1. The size data were expressed as $D_{0.1}$, $D_{0.5}$, $D_{0.9}$, which are equivalent spherical volume diameters at 10, 50, and 90% cumulative volume, respectively. The broadness of the size distribution, known as the span, equals $(D_{0.9}-D_{0.1})/D_{0.5}$.

Table I Precipitation Conditions for the Nano-Matrix Formulations

Precipitation conditions	Nano-matrix		
	A	B[a]	C[a]
Concentration of lysozyme solution (mg/mL)	40	60	40
Volume of lysozyme solution (mL)	50	50	75
Volume of isopropanol	450	450	425
Solvent : anti-solvent (i.e. lysozyme solution : isopropanol) volume ratio	1 : 9	1 : 9	1 : 5.7

[a] The resultant lysozyme nano-suspensions were diluted with additional isopropanol to 4 mg/mL to adjust the solid concentration in the sample before spray-drying

Atomic Force Microscopy

Particle surface roughness was quantified using atomic force microscopy (AFM) (Multimode Model MMAFMLN with Nanoscope IIIa controller; Veeco Metrology, Santa Barbara, CA, USA). The samples were dispersed onto carbon sticky tabs and imaged at a scan rate of 0.5 Hz using Veeco RTESP cantilevers (Veeco Metrology, Santa Barbara, CA) in tapping mode. Areas of 3 μm×3 μm were imaged with 512×512 sample points. The root mean square (RMS) roughness of three individual particles ($n=3$) was obtained over 510 nm×510 nm areas on the particles.

Colloidal Probe Microscopy

Inter-particulate cohesion was measured using colloidal probe microscopy. Individual particles were mounted onto the apex of V-shaped tipless atomic force microscopy (AFM) cantilevers (NP-0 silicon nitride cantilevers with gold reflective coating, nominal spring constant = 0.58 nN; Veeco Metrology, Santa Barbara, CA) using a micromanipulation technique described in Kumon *et al.* (2010) (36). The force of adhesion between each probe and particles mounted on a thermoplastic adhesive (Tempfix®; Plano, Wetzlar, Germany) was investigated using force-volume imaging. A 10 μm×10 μm area was scanned using the Multimode AFM described above with the following settings: 2 μm approach retraction cycle, 6.98 Hz cycle rate, and 60 nm constant compliance distance. The NanoScope IIIa software (Version 5.30r3.sr3; Veeco Metrology, Santa Barbara, CA) was employed for scan control and data collection. The adhesion force and topographical data matrices were derived using a custom-written software package. Topographic data were used to identify each particle, and individual force curves on the particle surfaces were analysed. Three probes ($n=3$) were made for each type of particle, and >140 force curves were collected per probe. For data analysis, the individual forces measured were assigned into bins of 5 nN in width from 0 to 250 nN. The frequency of forces within each bin was calculated to derive the median cohesion force ($F_{0.5}$).

In Vitro Aerosol Performance

The aerosol performance was assessed by dispersing 10 mg of powder into a Next Generation Impactor (NGI) under two conditions: i) from a Rotahaler® (Allen & Hanburys, Boronia, VIC, Australia) at 60 L/min of air flow for 4 s and ii) from an Aerolizer® (Novartis, North Ryde, NSW, Australia) at 100 L/min of air flow for 2.4 s. The dispersions were performed in triplicates. Size 3 hydroxypropyl methylcellulose capsules (Capsugel, West Ryde, NSW, Australia) were used for powder loading for both inhalers. To minimize particle bounce, the impactor stages were coated with silicon grease (Slipicone; DC Products, Waverley, VIC, Australia) before testing. After dispersion, the lysozyme deposits on each inhaler and NGI part was exhaustively washed with 5 mL deionised water. The solutions were then assayed by ultraviolet spectrophotometry at 280 nm. The cut-off diameters of the NGI stages at 100 L/min were calculated with the adjustment equations given in Appendix XII C of the British Pharmacopoeia (37). The fine particle fraction (FPF) was defined as the mass fraction of particles<5.0 μm with respect to the loaded dose in the capsules. One capsule was tested per run. Three runs were conducted for each powder under both dispersion conditions ($n=3$).

RESULTS

The Z-average diameters of Nanosuspensions A, B, and C measured by dynamic light scattering were 77.4±14.8, 545.7±319.8, and 79.8±6.5 nm, respectively. However, these were much larger than the size of the nano-units observed after spray-drying (see below). The nanoparticles must have been agglomerated in the suspensions; thus, the Z-average diameters did not reflect the primary sizes. The addition of one drop of Tween 80 to a 2 mL sample followed by 1-minute ultrasonication did not improve the sizing. The nanosuspensions were spray-dried to obtain micron-sized aggregates. The nano-matrix particles obtained for Formulations A, B, and C were comprised of nanoparticles of approximately 10, 20, and 70 nm in diameter, respectively, while the aqueous lysozyme solution produced smooth particles (Fig. 1). From the SEM images, the size of the primary nanoparticles increased with the aqueous lysozyme concentration and solvent-to-anti-solvent ratio.

These nano-matrix and smooth particles were comparable in physical size distribution ($D_{0.5}$ and span were 1.0–1.2 μm and 1.5–1.7, respectively; Table II) but possessed different surface roughness. The nano-matrix particles were likely to be formed from the grouping of the original agglomerates in the nanosuspensions and/or reorganisation of broken agglomerates, due to high shearing through the spray nozzle. The root mean square values from AFM showed an increasing order of roughness with spray-dried lysozyme particles being the least rough (21.5±2.8 nm), followed by Nano-matrix A (31.0±8.1 nm), B (39.8±3.5 nm) and C (53.8±9.8 nm). The nano-matrix roughness increased with the size of the primary nanoparticles, as corroborated by the SEM images.

Figure 2 shows the dispersion results with the Rotahaler® at 60 L/min and the Aerolizer® at 100 L/min, respectively. As expected, all powders performed

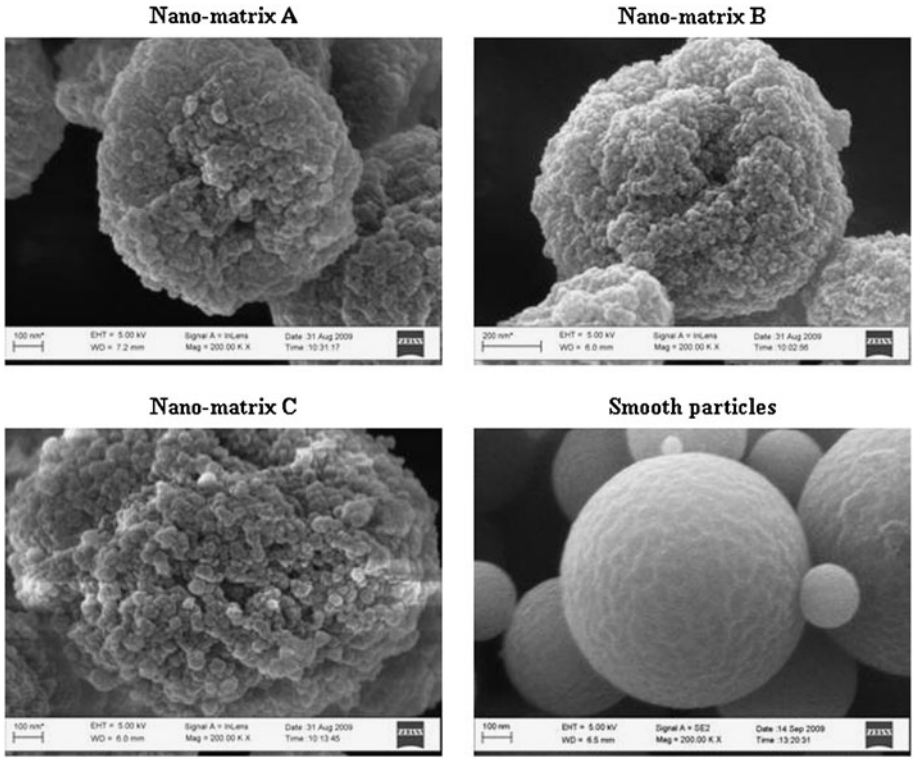

Fig. 1 SEM images of lysozyme nano-matrix and smooth particles.

better at the higher air-flow rate, with lower inhaler retention and more deposits on the lower stages. The relationship between the FPF and root mean square roughness is depicted in Fig. 3a. Spray-dried lysozyme was not efficiently dispersed using the Rotahaler® at 60 L/min, with a FPF of <20%. Increasing the surface roughness of the nano-matrix particles improved the FPF linearly, up to more than double the value of smooth lysozyme. The FPF of spray-dried lysozyme using the Aerolizer® at 100 L/min was relatively high at about 60%, which was further improved to about 80% with the nano-matrix particles (Fig. 3a). A slightly lower slope for the Aerolizer® at 100 L/min indicates that the dispersion was less dependent on surface roughness at the high dispersion condition. Furthermore, the nano-matrix particles always showed lower variations in the FPF than the smooth lysozyme.

To provide further insight into the performance of the nano-matrix particles, the cohesion force was measured using colloidal probe microscopy. The data showed that cohesion decreased with surface roughness (Fig. 4). The cohesion of Nano-matrix particles A, B, and C were similar, with B and C almost identical, while smooth lysozyme was markedly more cohesive (Fig. 4). At 100 L/min using the Aerolizer®, the FPF correlated closely with the median cohesion force (Fig. 3b). However, the correlation was poorer with the Rotahaler® at 60 L/min.

Table II Laser Diffraction Sizing Data

Formulation	Diameter (μm)			Span
	$D_{0.1}$	$D_{0.5}$	$D_{0.9}$	
Nano-matrix A	0.514	1.175	2.366	1.576
Nano-matrix B	0.473	1.032	1.997	1.478
Nano-matrix C	0.390	1.086	2.078	1.553
Smooth lysozyme	0.389	0.992	2.042	1.667

DISCUSSION

The Rotahaler® and Aerolizer® are single-dose commercial devices for proprietary inhalation formulations, with specific air-flow resistances of 0.04 and 0.07 $cmH_2O^{0.5}$/(L/min), respectively (38,39). The mean FPF of the commercial product Rotacaps® 400 generated from a Rotahaler® at 60 L/min was lower than that from a Cyclohaler® (another tradename for the Aerolizer®) at 90 L/min (40). This was the purpose for using the Rotahaler® at 60 L/min and the Aerolizer® at 100 L/min in the present study to represent a low and a high dispersion condition, respectively.

The aerosol performance of the nano-matrix and smooth lysozyme particles increased linearly with surface roughness in both dispersion conditions. This was attributed to the reduction in cohesive forces between the rough nano-matrix particles. These trends agree with those observed on corrugated BSA particles produced from spray-drying solutions.

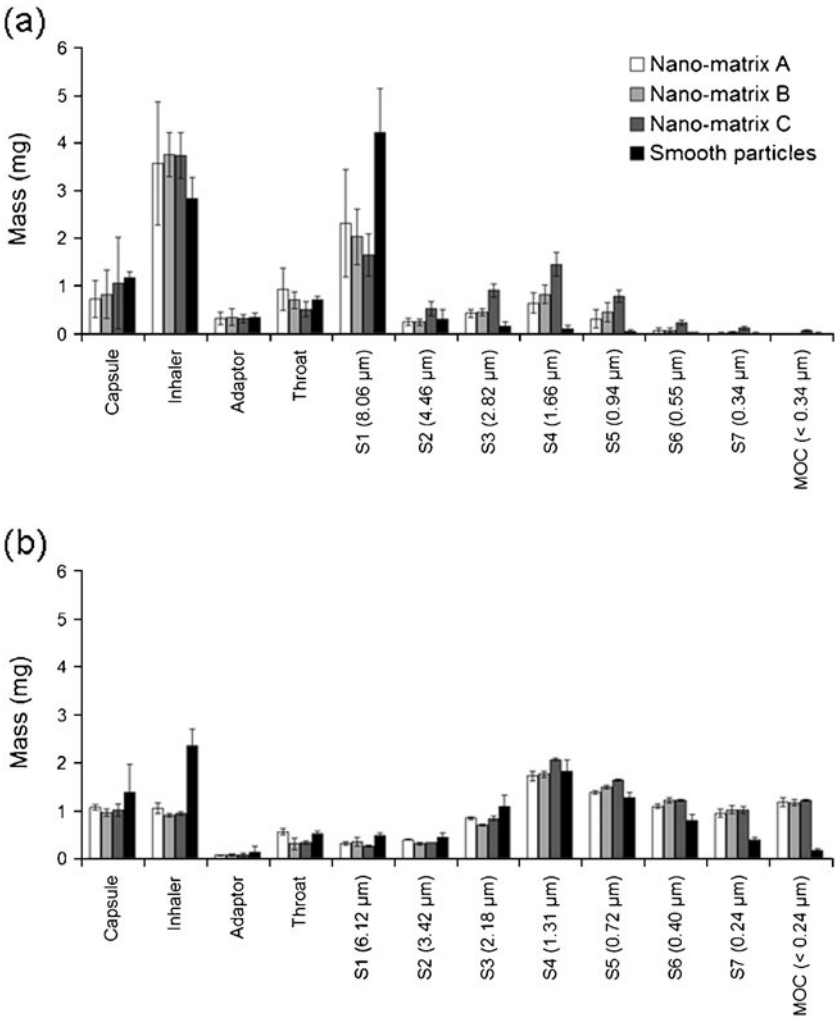

Fig. 2 Dispersion data of lysozyme nano-matrix and smooth particles using (**a**) the Rotahaler® at 60 L/min and (**b**) the Aerolizer® at 100 L/min. *Error bars* represent standard deviations ($n = 3$). S1 to S7 denote impactor stages 1 to 7, followed by the corresponding aerodynamic cutoff diameter in parentheses. MOC is the micro-orifice collector in the NGI.

The rougher BSA particles produced higher FPFs when dispersed alone (9–11) or from α-lactose monohydrate carriers (8). A similar trend was observed on dextran particles with different surface roughness (41). The fundamental reasons for these effects of nano-matrix and corrugated particles may be a reduction in the effective area available for contact and/or an increase in interparticulate distances due to surface asperities, subsequently reducing the van der Waals force (10,11). Furthermore, protrusions on the particle surface usually form the contact points between particles. It

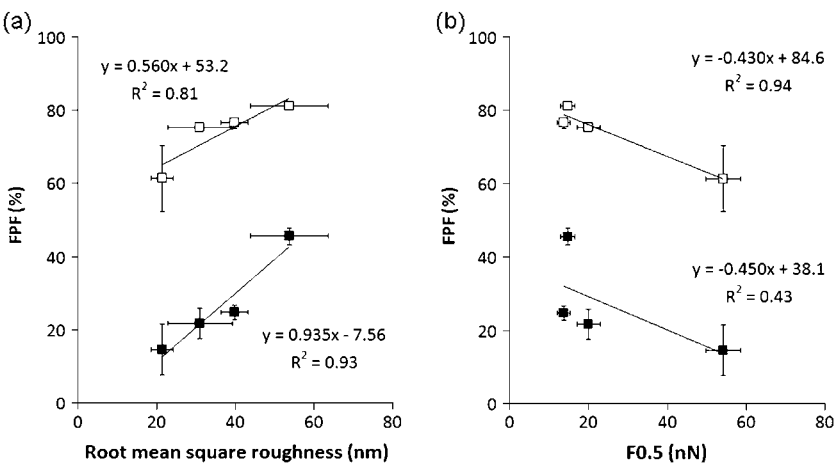

Fig. 3 Relationship between FPF and (**a**) root mean square roughness, (**b**) median cohesion force ((*black square*) Rotahaler® at 60 L/min, (*white square*) Aerolizer® at 100 L/min). *Error bars* represent standard deviations ($n = 3$).

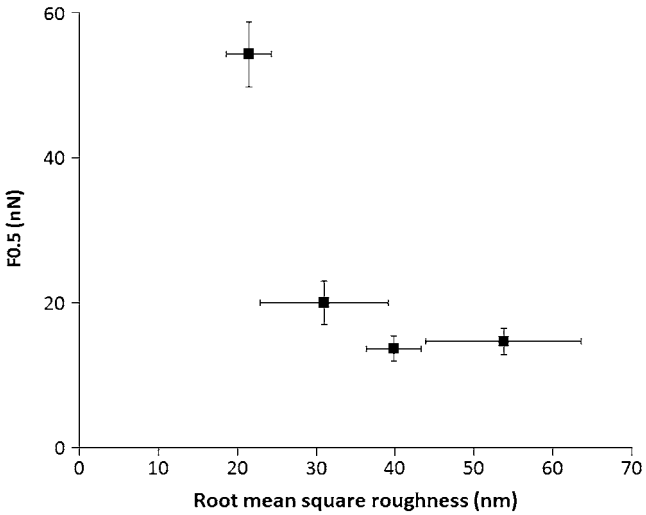

Fig. 4 Relationship between median cohesion force and root mean square roughness. *Error bars* represent standard deviations ($n = 3$)

has been demonstrated that adhesion increases with the diameter of protrusion (x_c) when x_c is > 100 nm (41). On the other hand, if x_c < 50 nm, such as those found on the nano-matrix particles in the present study, then adhesion increases with decreasing x_c (41). This agrees with the trends shown in Figs. 3 and 4. Besides having rough surfaces, the nano-matrix particles may also be porous. Any void inside the nano-matrix would reduce particle density, consequently lowering the aerodynamic diameter and contributing to the higher FPF (41,42).

It should be noted that the nano-matrix particles markedly decreased capsule and inhaler retention at 100 L/min. This is important from a product development viewpoint for lowering dose wastage. Interestingly, Fig. 2b shows substantial deposits on Stages 5, below which are of submicron size, suggesting fragmentation of the agglomerates by the inhaler and/or the NGI during the impaction. If fragmentation occurred in the inhaler, the inhaler retention should increase, as submicron particles are cohesive. The low retention of the nano-matrix particles (compared with the smooth particles) suggested fragmentation probably occurred in the NGI. The mass recovery was close to 100% of the loaded doses, so no significant amount of the nanoparticles escaped the impactor.

The magnitude of the median cohesion forces of lysozyme nano-matrix and smooth particles are comparable in magnitude to other spray-dried pharmaceutical powders measured with the same technique, generally between 15 and 200 nN (8,9,36,43). Compared to bovine serum albumin (BSA), lysozyme is a less cohesive protein. Although slightly rougher (root mean square roughness of 21.5 *vs* 14.1 nm), the smooth lysozyme particles are much less cohesive than the smooth BSA particles made in a previous study ($F_{0.5}$ of 54 *vs* 220 nN) (9). The slight increase in surface roughness of Nano-matrix A (root mean square roughness of 31.0 nm) greatly reduced $F_{0.5}$ to about 20 nN, while the corrugated BSA particle with root mean square roughness of 41.5 nm only reduced $F_{0.5}$ to about 110 nN.

The colloidal probe microscopy data clearly show that smooth lysozyme was significantly more cohesive than the nano-matrix particles (Fig. 4). This suggests that a small increase in surface roughness was enough to reduce cohesion significantly, and/or cohesion might be affected by the particle production method. The primary lysozyme nanoparticles were made by anti-solvent precipitation in a largely organic liquid mixture. On the other hand, the smooth particles were spray-dried directly from an aqueous solution. Due to the difference in hydrophilicity of the liquids, the orientation of the amino acid groups on the surface of the primary nanoparticles may orientate differently to those on the smooth lysozyme. This may in turn affect the physicochemical nature of the surface and hence cohesion.

Although the FPF and median cohesion force were closely correlated at 100 L/min using the Aerolizer®, the trend was poorer at 60 L/min with the Rotahaler®. This is because the dispersion of Nano-matrix C, the roughest one, was much higher than that predicted by the correlation. Although the cohesion of Nano-matrices B and C were similar, the extra roughness of C may have improved the dispersion via a non-cohesion mechanism, perhaps through additional mechanical interactions or improved aerodynamics. Therefore, its aerosol performance at the low dispersion condition could not be totally accounted for by the cohesion data. At 100 L/min using the Aerolizer®, the extra effects of this roughness may be masked by the high efficiency of the inhaler and air-flow rate. Hence, the aerosol performance closely followed the line of regression.

In conclusion, nano-matrix particles with controlled surface roughness were successfully produced from nanoparticular building blocks. Increasing their surface roughness

reduced cohesion, leading to higher and more reproducible FPF and lower inhaler retention.

ACKNOWLEDGMENTS

The work was financially supported by the Australian Research Council (Discovery Project 0985367).

REFERENCES

1. Chan H-K. Dry powder aerosol drug delivery—Opportunities for colloid and surface scientists. Colloids Surf, A. 2006;284–285:50–5.
2. Patton JS, Byron PR. Inhaling medicines: delivering drugs to the body through the lungs. Nat Rev Drug Discov. 2007;6:67–74.
3. Clark AR, Stevenson CL, Shire SJ. Formulation of proteins for pulmonary delivery. In: McNally EJ, Hastedt JE, editors. Protein formulation and delivery. New York: Informa Healthcare USA; 2008. p. 219–54.
4. Gonda I. Targeting by deposition. In: Hickey A, editor. Pharmaceutical inhalation aerosol technology. New York: Marcel Dekker; 2004. p. 65–88.
5. Hickey AJ, Mansour HM, Telko MJ, Xu Z, Smyth HDC, Mulder T, *et al.* Physical characterization of component particles included in dry powder inhalers. I. Strategy review and static characteristics. J Pharm Sci. 2007;96:1282–301.
6. Chan H-K, Clark A, Gonda I, Mumenthaler M, Hsu C. Spray dried powders and powder blends of recombinant human deoxyribonuclease (rhDNase) for aerosol delivery. Pharm Res. 1997;14:431–97.
7. Chan H-K. Inhalation drug delivery devices and emerging technologies. Expert Opin Ther Pat. 2003;13:1333–43.
8. Adi H, Traini D, Chan H-K, Young PM. The influence of drug morphology on the aerosolisation efficiency of dry powder inhaler formulations. J Pharm Sci. 2008;97:2780–8.
9. Adi S, Adi H, Tang P, Traini D, Chan H-K, Young PM. Microparticle corrugation, adhesion and inhalation aerosol efficiency. Eur J Pharm Sci. 2008;35:12–8.
10. Chew NYK, Chan H-K. Use of solid corrugated particles enhance powder aerosol performance. Pharm Res. 2001;18:1570–7.
11. Chew NYK, Tang P, Chan H-K, Raper JA. How much particle surface corrugation is sufficient to improve aerosol performance of powders? Pharm Res. 2005;22:148–52.
12. Rogueda PGA, Traini D. The nanoscale in pulmonary delivery. Part 2: formulation platforms. Expert Opin Drug Deliv. 2007;4:607–20.
13. Heyder J, Gebhart J, Rudolf G, Schiller CF, Stahlhofen W. Deposition of particles in the human respiratory tract in the size range 0.005–15 μm. J Aerosol Sci. 1986;17:811–25.
14. Tsapis N, Bennett D, Jackson B, Weitz DA, Edwards DA. Trojan particles: large porous carriers of nanoparticles for drug delivery. Proc Natl Acad Sci. 2002;99:12001–5.
15. Hadinoto K, Zhu K, Tan RBH. Drug release study of large hollow nanoparticulate aggregates carrier particles for pulmonary delivery. Int J Pharm. 2007;341:195–206.
16. Gómez-Gaete C, Fattal E, Silva L, Besnard M, Tsapis N. Dexamethasone acetate encapsulation into Trojan particles. J Control Release. 2008;128:41–9.
17. Loebenberg R, Finlay WH, Roa WH, Ely L. Effervescent powders for inhalation. US 2007/0031490 A1. 2007.
18. Ely L, Roa W, Finlay WH, Löbenberg R. Effervescent dry powder for respiratory drug delivery. Eur J Pharm Biopharm. 2007;65:346–53.
19. Azarmi S, Löbenberg R, Roa WH, Tai S, Finlay WH. Formulation and *in vivo* evaluation of effervescent inhalable carrier particles for pulmonary delivery of nanoparticles. Drug Dev Ind Pharm. 2008;34:943–7.
20. Finlay W, Orszanska H. Respirable dried powder formulation comprising drug loaded nanoparticles. WO 2006/130943 A1. 2006.
21. Azarmi S, Tao X, Chen H, Wang Z, Finlay WH, Löbenberg R, *et al.* Formulation and cytotoxicity of doxorubicin nanoparticles carried by dry powder aerosol particles. Int J Pharm. 2006;319:155–61.
22. Finlay WH, Roa W, Loebenberg R. Formulation of powder containing nanoparticles for aerosol delivery to the lungs. US 2005/0019270 A1. 2005.
23. Bailey MM, Gorman EM, Munson EJ, Berkland C. Pure insulin nanoparticle agglomerates for pulmonary delivery. Langmuir. 2008;24:13614–20.
24. El-Gendy N, Gorman EM, Munson EJ, Berkland C. Budesonide nanoparticle agglomerates as dry powder aerosols with rapid dissolution. J Pharm Sci. 2009;98:2731–46.
25. Plumley C, Gorman EM, El-Gendy N, Bybee CR, Munson EJ, Berkland C. Nifedipine nanoparticle agglomeration as a dry powder aerosol formulation strategy. Int J Pharm. 2009;369:136–43.
26. El-Gendy N, Berkland C. Combination chemotherapeutic dry powder aerosols via controlled nanoparticle agglomeration. Pharm Res. 2009;26:1752–63.
27. El-Gendy N, Berkland C. Combination nanoparticle agglomerates of fluticasone propionate and albuterol sulphate. In: Dalby RN, Byron PR, Peart J, Suman JD, Farr SJ, Young PM, editors. Respiratory drug delivery 2010. River Grove: Davis Healthcare International; 2010. p. 819–24.
28. Iskandar F, Lenggoro W, Xia B, Okuyama K. Functional nanostructured silica powders derived from colloidal suspensions by sol spraying. J Nanopart Res. 2001;3:263–70.
29. Chiou H, Chan H-K, Heng D, Prud'homme RK, Raper JA. A novel production method for inhalable cyclosporine A powders by confined liquid impinging jet precipitation. J Aerosol Sci. 2008;39:500–9.
30. Chiou H, Li L, Hu T, Chan H-K, Chen J-F, Yun J. Production of salbutamol sulfate for inhalation by high-gravity controlled antisolvent precipitation. Int J Pharm. 2007;331:93–8.
31. Glover WJ, Wan E, Yun JS, Chen J. A process for making micro-sized protein particles. WO 2009/020434 A1. 2009.
32. Berkland CJ, Shi L. Nanoclusters for delivery of therapeutics. US 7651770 B2. 2010.
33. Chen J-F, Zhou M-Y, Shao L, Wang Y-Y, Yun J, Chew NYK, et al. Feasibility of preparing nanodrugs by high-gravity reactive precipitation. Int J Pharm. 2004;269:267–74.
34. Hu T, Chiou H, Chan H-K, Chen J-F, Yun J. Preparation of inhalable salbutamol sulphate using reactive high gravity controlled precipitation. J Pharm Sci. 2008;97:944–9.
35. Instruction Manual ULTRA *plus* Field Emission Scanning Electron Microscope, Carl Zeiss NTS GmBH, Oberkochen, Germany, 2008.
36. Kumon M, Kwok PCL, Adi H, Heng D, Chan H-K. Can low-dose combination products for inhalation be formulated in single crystalline particles? Eur J Pharm Sci. 2010;40:16–24.
37. British Pharmacopoeia Appendix XII C, Spottiswoode, London, 2010.
38. Clark AR, Hollingworth AM. The relationship between powder inhaler resistance and peak inspiratory conditions in healthy volunteers—Implications for *in vitro* testing. J Aerosol Med. 1993;6:99–110.
39. Molimard M, Till D, Stenglein S, Singh D, Krummen M. Inhalation devices for long-acting β_2-agonists: Efficiency and ease of use of dry powder formoterol inhalers for use by patients with asthma and COPD. Curr Med Res Opin. 2007;23:2405–13.

40. Srichana T, Martin GP, Marriott C. Dry powder inhalers: the influence of device resistance and powder formulation on drug and lactose deposition *in vitro*. Eur J Pharm Sci. 1998;7:73–80.
41. Weiler C, Egen M, Trunk M, Langguth P. Force control and powder dispersibility of spray dried particles for inhalation. J Pharm Sci. 2010;99:303–16.
42. Heng D, Tang P, Cairney JM, Chan H-K, Cutler DJ, Salama R, *et al*. Focused-ion-beam milling: a novel approach to probing the interior of particles used for inhalation aerosols. Pharm Res. 2007;24:1608–17.
43. Adi H, Young PM, Chan H-K, Agus H, Traini D. Co-spray-dried mannitol-ciprofloxacin dry powder inhaler formulation for cystic fibrosis and chronic obstructive pulmonary disease. Eur J Pharm Sci. 2010;40:239–47.